Large-Signal-Network-Analyzer Phase Calibration on an Arbitrary Grid

Aric Sanders[1], Dylan F. Williams[2], Joshua M. Kast[3], Kate A. Remley[1], Robert D. Horansky[1]
[1]Department of Physics, University of Colorado, Boulder, CO USA
[2]National Institute of Standards and Technology, Boulder, CO USA
[3]Department of Electrical Engineering, Colorado School of Mines, Golden, CO USA
aric.sanders@nist.gov, dylan.williams@nist.gov

***Abstract*— We have developed a method for improving the synchronization of large-signal network analyzers and transferring "cross-frequency" phase calibrations from a calibrated sampling oscilloscope to the large-signal network analyzer on an arbitrary frequency grid. The approach can be applied to the measurement of modulated signals and other waveforms on arbitrary and fine frequency grids. This translates into the ability to measure complex and arbitrarily long signals traceably with high dynamic range.**

***Keywords*—phase calibration, oscilloscope, arbitrary waveform generator, large-signal network analyzer, wireless system.**

I. Introduction

We present a practical and accurate way of calibrating the "cross-frequency" phases of large-signal network analyzer (LSNA) measurements on arbitrary, irregularly-spaced, and fine frequency grids. The method overcomes spacing and placement limitations of the calibration frequency grids inherent in the current approach to LSNA calibration, which uses comb generators to calibrate the cross-frequency phases of large-signal network analyzer measurements. The method is based on commercially available instrumentation.

Large-signal network analyzers add power and cross-frequency phase calibrations to the conventional vector-network-analyzer (VNA) scattering-parameter calibration. These additional calibration steps allow the LSNA to measure not only scattering parameters, but the amplitude and phase of each of the forward and backward waves at the ports of the LSNA [1]. LSNAs find applications in nonlinear device characterization [1-3], modulated-signal characterization [4] and the characterization of devices excited by modulated signals [5].

While LSNAs are available in both sampler-based and mixer-based architectures [6], the mixer-based architectures are more common and typically offer higher dynamic range. Mixer-based architectures usually make use of comb generators to provide a constant set of constant-phase reference tones for the LSNA as well as to calibrate the cross-frequency phase of the LSNA [1, 2]. However, this limits the LSNA to measurements on uniform commensurate frequency grids. As the frequency spacing is reduced, the total power available in the grid is also reduced, limiting the upper frequency limit of the LSNA.

There has been considerable work on creating finer LSNA frequency grids with varying degrees of success. Recently, Verbeyst, et al. [7] and Vanden Bossche, et al. [8] used lower-frequency pseudo-random bit sequences (PRBS) to trigger the comb, moving energy from the harmonics of the fundamental to a fine grid around the fundamental and a few harmonics of that fundamental. Verspecht, et al. [9] used a similar approach to generate finely-spaced tones with a chirped input. While this allows for finer frequency grids, these approaches do not have complete flexibility in the choice of the grid and are still limited in the total number and bandwidth of frequency points over which the LSNA can be calibrated and perform measurements.

Hale, et al. [10] added a band-pass filter and amplifier after the comb generator to boost the power available to the LSNA over the bandwidth of the filter and amplifier. This is useful for band-limited signals but cannot be applied to perform measurements on arbitrary frequency grids.

Zhang, et al. [11, 12] proposed a multistep calibration process that stitches multisine signals together in postprocessing to perform broadband calibrations at fine tone spacings. However, we have found that stitched multistep calibration processes degrade calibration accuracy, particularly when they contain many stitched frequency bands.

Here, we circumvent these limitations by 1) using an arbitrary waveform generator (AWG) to synchronize the measurement apparatus using a method similar to that used in [13, 14] and 2) direct calibration of the LSNA with a calibrated oscilloscope following the approach of [15]. This offers a practical and accurate way of transferring oscilloscope cross-frequency phase calibrations to large-signal network analyzers on arbitrary (including arbitrarily fine) frequency grids.

Our approach has the following advantages:

- The method is applicable to any frequency grid that can be generated by the AWG.
- The phase lock of the measurement apparatus can be implemented at high frequencies (10 GHz in our case), lowering phase noise.
- The AWG can provide power at only the frequencies of interest, greatly increasing the signal-to-noise ratio compared to standard comb-based approaches and lifting restrictions on the upper frequency limit and tone spacing.
- The measurement apparatus can be operated at the highest frequency that can measured by a calibrated oscilloscope, currently about 110 GHz.
- The LSNA can be calibrated with single-tone signals on an arbitrary frequency grid for slightly more than a cycle, making them fast and easy to measure on the sampling oscilloscope.

- The sampling oscilloscope can be calibrated directly with a calibrated photodiode [16-18], eliminating comb generators from the traceability path.
- In theory, the measurement apparatus could be directly calibrated and operated on wafer to the highest frequency at which electro-optic sampling can be used to provide the phase calibration in place of the oscilloscope, currently about 1 THz.

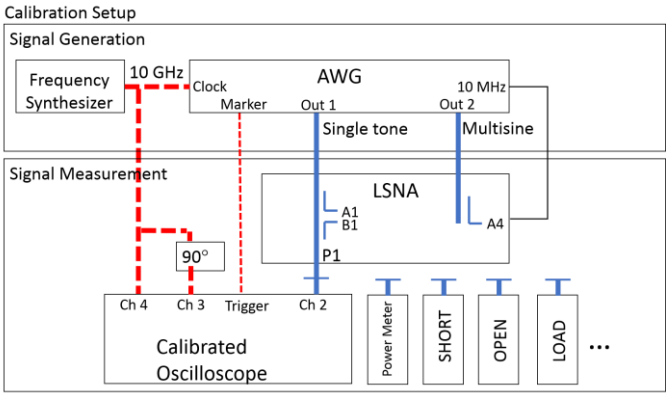

Fig. 1. The measurement apparatus during calibration. Once calibrated, the oscilloscope, power meter and scattering-parameter calibration standards can be removed and the LSNA used to perform measurements on P1.

II. Measurement Apparatus

Figure 1 shows the measurement apparatus during calibration. During calibration, the AWG provides sinusoids to the LSNA at Out 1. These are used to perform the standard frequency-point-by-frequency-point LSNA scattering-parameter and power calibrations on port 1 (P1) of the LSNA. These sinusoids from the AWG Out 1 are also used to provide a sinusoid at each frequency that can be measured by both the oscilloscope and the LSNA, a process in which the oscilloscope need only measure one cycle of the sinusoid. A comparison of the phases of the sinusoid measured by the LSNA and the oscilloscope is used to transfer the oscilloscope's cross-frequency phase calibration to the LSNA.

The AWG in Fig. 1 provides synchronization for the measurement apparatus in a similar manner to [13, 14]. It generates a 10 MHz or other lock signal for the VNA and the oscilloscope trigger signal. The frequency synthesizer also creates the precision 10 GHz IQ reference signals for correcting for time-base-distortion for the oscilloscope using the methods of [19-21] and the clock signal for the AWG.[1]

After calibration with the oscilloscope, power meter, and scattering-parameter calibration standards (shown as an open, short and load in the figure), these calibration standards can be disconnected and the LSNA used to measure modulated forward-wave and backward-wave signals on port 1 of the LSNA (labeled P1 in Fig. 1). These signals on P1 can be

[1] The frequency synthesizer could be eliminated by using an AWG with more channels to create these 10 GHz IQ reference signals.

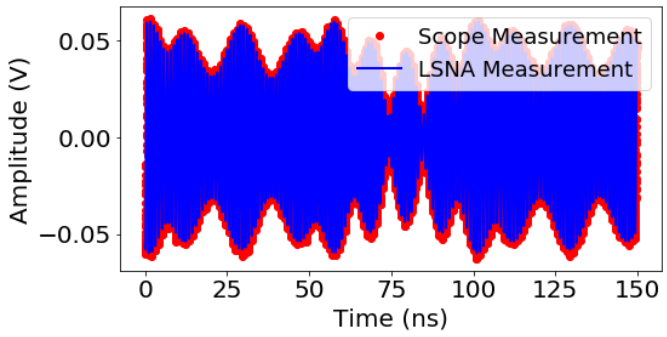

(a)

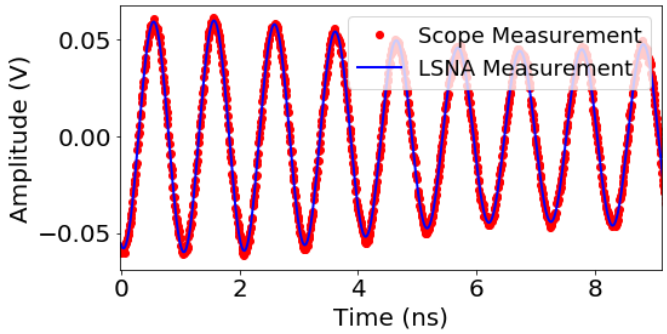

(b)

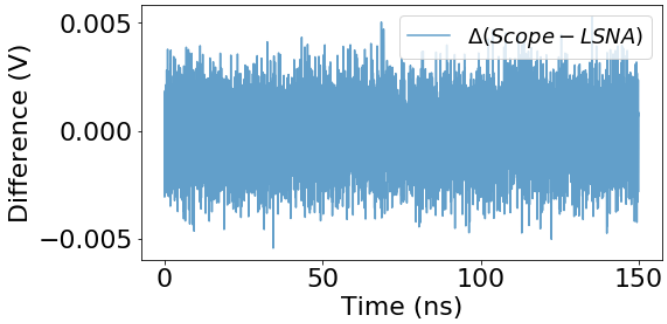

(c)

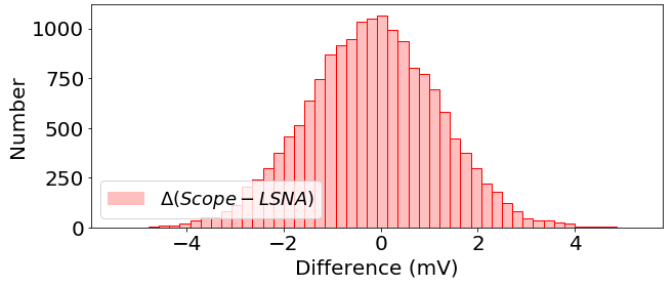

(d)

Fig. 2. Time-domain comparison of the 11-tone 10 MHz multisine measured by the LSNA and oscilloscope. (a) Signal envelope. (b) Closeup of the signal. The time-base correction algorithm moves points off of a regular grid. (c) The difference of the scope and LSNA measurements. (d) Histogram of the difference of the scope and LSNA measurements, with a mean of 0.2 mV and standard deviation of 1.4 mV.

generated by the AWG on Out 1 or externally by other instruments or devices that are locked to the frequency synthesizer or AWG.

During both calibration and measurement, the AWG provides a multisine reference signal on Out 2 for the LSNA with tones at each of the frequencies of interest. This signal serves as a phase reference for the LSNA as it makes measurements. The purpose of this phase reference is to provide the LSNA with a set of unknown but stable tones to use as a reference for other signals it measures. In postprocessing each phase measured by the LSNA on P1 is referred to the fixed phase of the tone at the same frequency generated on the AWG's Out 2, minimizing the need accuracy in the LSNA's 10 MHz reference. To minimize distortion in the LSNA, we used a Schroeder multisine [22] to keep the peak-to-average power ratio low.

III. Measurement Results

We first illustrate the technique on a multisine measurement where the tone spacing corresponds to the standard minimum spacing of commercially available comb generators, 10 MHz. This allows easy comparison to the sampling oscilloscope calibrated measurements. Then, we illustrate the method on a 25 kHz grid, which requires an exceedingly long sampling oscilloscope measurement (40 µs total time) and showcases the strength of our method.

We first calibrated the oscilloscope with a photodiode calibrated on the National Institute of Standards and Technology's electro-optic sampling (EOS) system [16-18]. We then used the procedure described in the previous section to calibrate the LSNA with scattering-parameter artifacts, a power meter, and the EOS-calibrated oscilloscope, from which we transferred the phase calibration to the LSNA. Finally, we used the apparatus to measure several multisines centered at 1 GHz.

A. 10 MHz Multisine Measurement Example

After completing the calibrations, we generated an 11-tone Schroeder multisine on Out 1 of the AWG and measured that multisine with both the LSNA and the calibrated oscilloscope. Figure 2 compares the direct measurement of the signal with the oscilloscope after time-base and mismatch corrections to the measurement performed by the LSNA after transformation to the time domain. Figure 2 (a) shows that the two instruments measure nearly the same 100 ns long envelope. Figure 2 (b) shows a closeup view of the actual signals measured by the two instruments. The two signals overlap to such a great extent that it is almost impossible to tell the difference in the plot.

Figure 2 (c) shows that the difference of the two measurements is small and has no discernible structure. The histogram in Fig 2 (d) shows the difference to be approximately Gaussian with a mean of 0.2 mV and a standard deviation of 1.4 mV, much smaller than the roughly 100 mV peak-to-peak amplitude of the signal, identical to the residual distribution of a multisine fit of the oscilloscope and close to the 1.3 mV rms noise specification of the manufacturer.

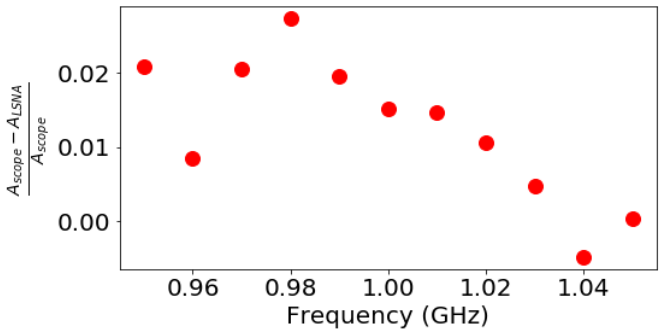

(a)

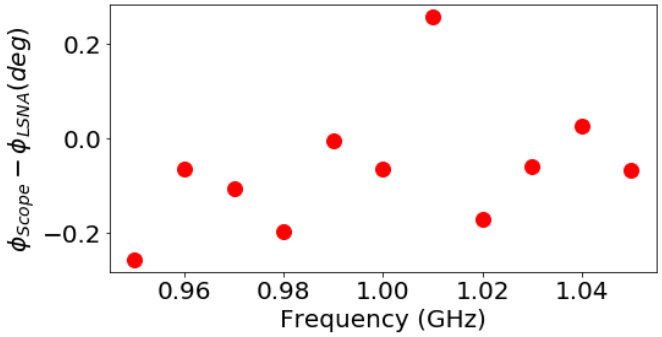

(b)

Fig. 3. Frequency-domain comparison of the 11-tone 10 MHz multisine measured by the LSNA and oscilloscope. (a) Fractional difference in the voltage measurements. (b) Phase difference of the two measurements.

We also examined the results in the frequency domain to better assess the consistency of the LSNA and oscilloscope power-meter calibrations and the accuracy of the transfer of the oscilloscope's cross-frequency phase calibration to the LSNA. Figure 3 (a) shows that the fractional difference of the forward-wave voltage measurements made by the oscilloscope (A_{Scope}) and the LSNA (A_{LSNA}) are within about 2 % of each other.

Figure 3 (b) shows that the differences in phase measured by the LSNA and oscilloscope differ by less than a quarter of a degree, despite that fact that the phase at each frequency point in the calibration was calibrated separately. These phase differences correspond to a drift of less than 1 ps in the synchronization of the measurement apparatus.

B. 25 kHz Multisine Measurement Example

We also created an 11-tone Schroeder multisine on the AWG with a 25 kHz tone spacing. Figure 4 (a) compares the envelope of the signal we uploaded to the AWG and measured with the LSNA. The time offset is due to the various hardware between the AWG's converters and the LSNA's calibration reference plane at P1. This 25 kHz narrow tone spacing resulted in a signal with a 40 µs repetition rate, too long to measure accurately with our sampling oscilloscope. However, because of the way that the measurement apparatus is synchronized by the AWG, we were able to measure portions of the signal with our oscilloscope and compare those to the temporal signal reconstructed by the LSNA, as shown in Fig. 4 (b). Here again,

the comparison is excellent, even at the narrow tone spacing of this multisine.

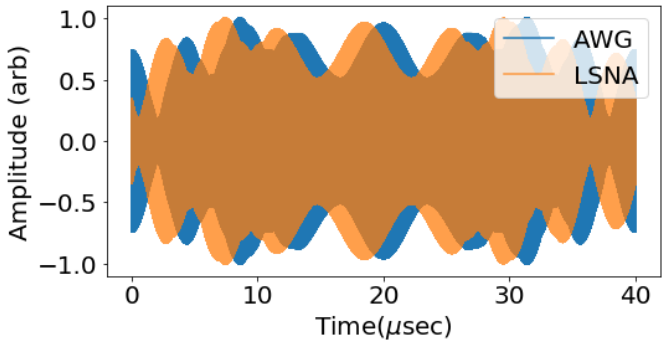

(a)

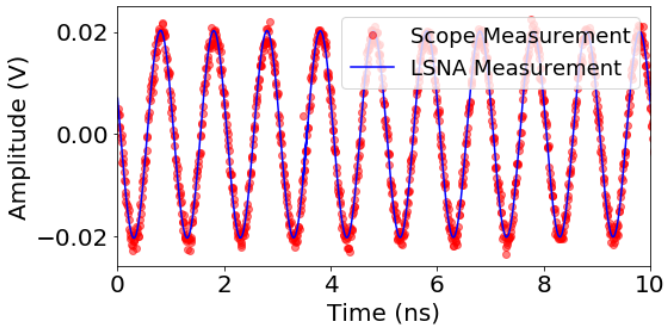

(b)

Fig. 4. Time-domain comparison of an 11-tone 25 kHz multisine. (a) Temporal envelope uploaded to AWG and measured by LSNA, offset caused by path delay. (b) Time-domain comparison of LSNA and oscilloscope measurements. The time-base correction algorithm reassigns time points based on the 10 GHz signal from the frequency synthesizer.

IV. Conclusion

We described a fast, accurate and practical way of calibrating the cross-frequency phases of LSNAs on any frequency grid that can be generated with an AWG and measuring any repetitive communications signal that we can create with the instrument. We used an AWG to synchronize the measurements and then transferred the cross-frequency phase calibration of the oscilloscope to the LSNA.

We verified the approach with two 11-tone multisines having 10 MHz and 25 kHz tone spacings, demonstrating that we could transfer the phase calibration of the oscilloscope to the LSNA over a wide range of tone spacing to within accuracy of a fraction of a degree.

References

[1] J. Verspecht, "Large-Signal Network Analysis," *IEEE Microwave Magazine,* vol. 6, no. 4, pp. 82-92, 2005.

[2] J. Verspecht, "Calibration of a Measurement System for High Frequency Nonlinear Devices," *Ph.D.Thesis, Free University of Brussels,* 1995.

[3] J. Verspecht, D. F. Williams, D. Schreurs, K. A. Remley, and M. D. McKinley, "Linearization of large-signal scattering functions," *IEEE Transactions on Microwave Theory and Techniques,* vol. 53, no. 4, pp. 1369-1376, 2005.

[4] N. B. Carvalho, K. A. Remley, D. Schreurs, and K. G. Card, "Multisine signals for wireless system test and design [Application Notes]," *IEEE Microwave Magazine,* vol. 9, no. 3, pp. 122-138, 2008.

[5] J. Verspecht, F. Verbeyst, and M. Vanden Bossche, "Network Analysis Beyond S-parameters: Characterizing and Modeling Component Behaviour under Modulated Large-Signal Operating Conditions," *ARFTG Conference Digest,* vol. 56, pp. 1-4, 2009.

[6] W. V. Moer and L. Gomme, "NVNA versus LSNA: enemies or friends?," *IEEE Microwave Magazine,* vol. 11, no. 1, pp. 97-103, 2010.

[7] F. Verbeyst, M. V. Bossche, and G. Paillonc, "Next-generation comb generators for accurate modulated measurements," in *81st ARFTG Microwave Measurement Conference*, 2013, pp. 1-4.

[8] M. V. Bossche, F. Verbeyst, and A. Samant, "Traceable phase calibration of a wide-bandwidth microwave Vector Signal Analyzer," in *2015 IEEE MTT-S International Microwave Symposium*, 2015, pp. 1-4.

[9] J. Verspecht, "Generation and measurement of a millimeter-wave phase dispersion reference signal based on a comb generator," in *2016 IEEE MTT-S International Microwave Symposium (IMS)*, 2016, pp. 1-4.

[10] P. D. Hale, K. A. Remley, D. F. Williams, J. A. Jargon, and C. M. J. Wang, "A compact millimeter-wave comb generator for calibrating broadband vector receivers," in *2015 85th Microwave Measurement Conference (ARFTG)*, 2015, pp. 1-4.

[11] Y. Zhang, Z. He, H. Li, and M. Nie, "Dense Spectral Grid NVNA Phase Measurements Using Vector Signal Generators," *IEEE Transactions on Instrumentation and Measurement,* vol. 63, no. 12, pp. 2983-2992, 2014.

[12] Y. Zhang *et al.*, "Characterization for Multiharmonic Intermodulation Nonlinearity of RF Power Amplifiers Using a Calibrated Nonlinear Vector Network Analyzer," *IEEE Transactions on Microwave Theory and Techniques,* vol. 64, no. 9, pp. 2912-2923, 2016.

[13] K. A. Remley, P. D. Hale, D. F. Williams, and C. M. Wang, "A precision millimeter-wave modulated-signal source," in *Microwave Symposium Digest (IMS), 2013 IEEE MTT-S International*, 2013, pp. 1-3.

[14] A. S. Boaventura, D. F. Williams, G. Avolio, and P. D. Hale, "Traceable Characterization of Broadband Pulse wavefroms Suitable for Cryogenic Josephson Voltage Applications," in *2018 IEEE/MTT-S International Microwave Symposium - IMS*, 2018, pp. 1176-1179.

[15] A. Aldoumani, P. J. Tasker, R. S. Saini, J. W. Bell, T. Williams, and J. Lees, "Operation and calibration of VNA-based large signal RF I-V waveform measurements system without using a harmonic phase reference standard," in *81st ARFTG Microwave Measurement Conference*, 2013, pp. 1-4.

[16] T. S. Clement, P. D. Hale, D. F. Williams, C. M. Wang, A. Dienstfrey, and D. A. Keenan, "Calibration of Sampling Oscilloscopes with High-Speed Photodiodes," *IEEE Trans.Microw.Theory Techn.,* vol. 54, no. 8, pp. 3173-3181, 2006.

[17] P. D. Hale *et al.*, "Traceable waveform calibration with a covariance-based uncertainty analysis," *IEEE Trans.Instrum.Meas.,* vol. 58, pp. 3554-3568, 2009.

[18] P. D. Hale *et al.*, "Traceability of high-speed electrical waveforms at NIST, NPL, and PTB," in *2012 Conference on Precision electromagnetic Measurements*, 2012, pp. 522-523.

[19] C. M. Wang, P. D. Hale, and K. J. Coakley, "Least-squares estimation of time-base distortion of sampling oscilloscopes," *IEEE Trans.Instrum.Meas.,* vol. 48, no. 6, pp. 1324-1332, 1999.

[20] C. M. J. Wang, P. D. Hale, J. A. Jargon, D. F. Williams, and K. A. Remley, "Sequential Estimation of Timebase Corrections for an Arbitrarily Long Waveform," *IEEE Transactions on Instrumentation and Measurement,* vol. 61, no. 10, pp. 2689-2694, 2012.

[21] H. C. Reader, D. F. Williams, P. D. Hale, and T. S. Clement, "Comb-Generator Characterization," *IEEE Transactions on Microwave Theory and Techniques,* vol. 56, no. 2, pp. 515-521, 2008.

[22] M. Schroeder, "Synthesis of low-peak-factor signals and binary sequences with low autocorrelation (Corresp.)," *IEEE Transactions on Information Theory,* vol. 16, no. 1, pp. 85-89, 1970.